Hormonally regulated myogenic miR-486 influences sex-specific differences in cancer-induced skeletal muscle defects

Ruizhong Wang[1], Poornima Bhat-Nakshatri[1], Xiaoling Zhong[1], Teresa Zimmers[1,3], and Harikrishna Nakshatri[1,2,3 *]

[1]Department of Surgery, Indiana University School of Medicine, Indianapolis, IN 46202, USA

[2]Department of Biochemistry and Molecular Biology, Indiana University School of Medicine, Indianapolis, IN 46202, USA

[3]Richard L Roudebush VA Medical Center, Indianapolis, IN 46202, USA

Funding: Department of Veterans Affairs merit award BX002764 and Research Career Scientist Award IK6 BX005244 funded this study (to HN).

Disclosure summary: Authors have no conflict of interest to declare.

***Corresponding Author:** Harikrishna Nakshatri, BVSc., PhD

C218C, 980 West Walnut St.

Indianapolis, IN 46202, USA

317 278 2238

hnakshat@iupui.edu

Reprint requests: Harikrishna Nakshatri (hnakshat@iupui.edu)

ABSTRACT

Cancer-induced skeletal muscle defects show sex-specific differences in severity with men performing poorly compared to women. Hormones and sex chromosomal differences are suggested to mediate these differences, but the functional skeletal muscle markers to document these differences are unknown. We show that the myogenic microRNA miR-486 is a marker of sex-specific differences in cancer-induced skeletal muscle defects. Cancer-induced loss of circulating miR-486 was more severe in men with bladder, lung and pancreatic cancers compared to women with the same cancer types. In syngeneic model of pancreatic cancer, circulating and skeletal muscle loss of miR-486 was more severe in male mice compared to female mice. Estradiol (E2) and the clinically used selective estrogen receptor modulator toremifene increased miR-486 in undifferentiated and differentiated myoblast cell line C2C12 and E2-inducible expression correlated with direct binding of estrogen receptor alpha (ERα) to the regulatory region of *miR-486* gene. E2 and toremifene reduced the actions of cytokines such as myostatin, TGFβ and TNFα, which mediate cancer-induced skeletal muscle wasting. E2 and toremifene treated C2C12 myoblast/myotube cells contained elevated levels of active AKT with corresponding decrease in the levels of its negative regulator PTEN, which is a target of miR-486. We propose an ERα:E2-miR-486-AKT signaling axis, which reduces the deleterious effects of cancer-induced cytokines/chemokines on skeletal muscle mass and/or function.

Keywords: estradiol, miR-486, breast cancer, systemic effects, skeletal muscle

Introduction

Sex-specific differences in severity of cachexia have been recognized for a number of years and molecular basis for these differences are just beginning to be explored (1). Men with cancer compared to women with the same cancer types show greater loss of grip strength, skeletal muscle depletion and cancer-related fatigue as well as distinct transcriptomic changes in skeletal muscle (1,2). These differences have clinical impact with respect to progression free and overall survival. For example, male veterans with pulmonary hypertension, often with cachexia or functional limitations, have poorer outcome than women (3). Men with aggressive B cell lymphoma with accompanying sarcopenia have worse outcome than women with the same disease and accompanying sarcopenia. These sex-specific differences in cancer-induced skeletal defects have been attributed to two factors: hormonal and chromosomal factors (4,5). For example, sex dimorphism in immune response, which can indirectly effect skeletal muscle function, is attributed to sex chromosomes (6). The potential role of hormones in skeletal muscle function is just beginning to be addressed (2). Most of our current knowledge is focused on the action of steroid and growth hormones on skeletal muscle (7). For example, estradiol (E2) directly lowers mitochondrial membrane microviscosity and improves bioenergetics function in skeletal muscle, independent of its function as a ligand for the estrogen receptor (8), indicating the role of E2 in skeletal muscle function (9).

Myogenesis is a tightly controlled process requiring coordinated activity of various transcription factors that maintain stemness or trigger differentiation of skeletal muscle stem cells (MuSCs) (10). MicroRNAs control the levels of myogenic transcription factors at various steps of myogenesis cascade. For example, differentiation of myoblasts to myotubes involves selective decrease in the expression of myocardin-related transcription factor A (MRTF-A), which is mediated by the differentiated skeletal muscle-enriched miR-486 (11).

Various diseases associated with skeletal muscle defects including Duchenne Muscular Dystrophy (DMD) and cachexia are associated with deregulation of this tightknit myogenic transcription factor-microRNA network. Short-term and long-term hindlimb immobilization with accompanying muscle dysfunction and subsequent muscle reloading for recovery are associated with reduction and regain of skeletal muscle miR-486 expression, respectively, suggesting a critical role of miR-486 in skeletal muscle physiology (12). Reduction in skeletal muscle miR-486 and amelioration of skeletal muscle defects upon restoration of miR-486 expression have been reported in DMD models (13). For example, muscle-specific transgenic overexpression of miR-486 in DMD and aged mice improves sarcolemmal integrity, increases myofiber size, and enhances muscle performance such as increased muscle contraction force and grip strength (14). Disruption in myofiber architecture, decreased myofiber size, decreased locomotor activity, increased cardiac fibrosis, and metabolic defects were observed in miR-486 knock-out mice (15) Thus, miR-486 is an integral part of the myogenesis program (11,16). We had previously demonstrated selective decrease in skeletal muscle miR-486 in transgenic models of breast cancer and pharmacologic approaches to restore skeletal muscle miR-486 expression and overcome cancer-induced skeletal muscle defects (17,18). Furthermore, we reported that reduced levels of skeletal muscle miR-486 in cancer models correlate with reduced levels of circulating miR-486 and proposed that circulating miR-486 can be used as a biomarker of cancer-induced systemic effects (17,18).

DMD, which is a X-linked, recessive, muscle-wasting disease, predominantly affects males. In experimental models of DMD, despite male and female mice having the same genetic aberration, skeletal muscle defects were more severe in males compared to females at six months age, but these defects were more severe in females than males at 20-months (19). Thus, hormonal factors, independent of mutations in dystrophin gene, impact skeletal muscle

function in DMD cases. Because of these observations in DMD models, known sex-specific differences in severity of cancer-induced cachexia and our observation of loss of miR-486 in skeletal muscle in cancer models, this study investigated whether there are sex-specific differences in cancer-induced loss of miR-486 in skeletal muscle, which can be easily recapitulated by measuring circulating miR-486 levels, and whether E2 plays any role in regulating miR-486 expression. We demonstrate that miR-486 is an E2-regulated microRNA and E2 or selective estrogen receptor modulator (SERM) toremifene can reverse cancer-induced defects in skeletal muscle cells including restoring miR-486 expression and blocking the actions of pro-cachectic cytokines such as TNFα, TGFβ, and myostatin.

Materials and Methods

Human plasma sample processing and miRNA extraction.

The Indiana University Institutional Review board approved the use of human sera/plasma samples. Plasma from healthy volunteers were obtained from the Susan G. Komen for the Cure Normal Breast Tissue Bank (KTB) at the IU Simon Comprehensive Cancer Center as well as from Hoosier Cancer Research Network (HCRN) after obtaining informed consent. Plasma samples from cancer patients were obtained from HCRN. All samples were collected in accordance with standard operating procedure described in websites of KTB and HCRN. Qiagen miRNeasy Serum/Plasma kit (Qiagen, Valencia, CA, USA) was used to isolate miRNAs from 200 µL of human plasma. Complete miRNA extraction procedure has been described in our previous publications (20,21).

Animal model of pancreatic tumor and E2 pellet implantation.

National Institutes of Health regulations concerning the use and care of experimental animals were followed while conducting animal studies and the Indiana University School of Medicine animal use committee approved this study. KPC32908 cell line, derived from a genetically engineered mouse model of pancreatic ductal adenocarcinoma (PDAC) (22), was used to generate the orthotopic pancreatic tumors as described previously (23) with some modifications. Briefly, 5 x 10^4 KPC32908 cells were injected into the pancreas of 15-week-old wild-type C57BL/6 mice purchased from Jackson Laboratory. On day 15 post injection when the mice reached the designated endpoint due to tumor growth and cachexia, blood and tissues including skeletal muscles were collected and processed for microRNA analyses. The sham-operated mice with the same age and sex were used as controls.

For E2 pellet implantation experiment, 5 males ~6-weeks old C57BL/6j mice were implanted with 0.72mg 60-days slow release E2 pellet (Innovative Research of America, Cat# SE-121) under the skin. At day 8 post implantation, mice were sacrificed for blood and tibialis anterior skeletal muscle harvest, followed by RNA extraction and miR-486 qPCR quantification. Control male mice of same age received similar implantation procedure without E2 pellets.

Cell culture and treatments.

Mouse myoblast C2C12 cells were maintained in high-glucose DMEM with 10% FBS and 1% penicillin/streptomycin. To obtain differentiated myotubes, C2C12 cells were allowed to reach 90% confluence, then switched to differentiation medium (high-glucose DMEM with 2% horse serum and 1% penicillin/streptomycin) for seven days. Undifferentiated C2C12 myoblasts and differentiated myotubes were rinsed in PBS and maintained in MEM (Minimum Essential Medium) with 5% charcoal-stripped serum (CSS) and 1% penicillin/streptomycin for three days, then treated by vehicle, E2 (10^{-10} M),

toremifene (Selleckchem, Cat# S1776; 10^{-6} M) or combination of E2 and toremifene for three, six, and 24 hours respectively. In the six hours treatment with E2 or toremifene, myostatin (Millipore, Cat# 345762; 100ng/ml) was added 15 minutes prior to cell harvest for protein analysis. For miR-486 level analysis, in the six hours treatment with E2 or toremifene, myostatin (100ng/ml), TNFα (BD Pharmingen, Cat#554589; 20ng/ml) and TGFβ (R&D system, Cat#7666-MB; 20ng/ml) were added one hour after E2 or toremifene addition to the media (five hours exposure prior to cell harvest).

In myotube formation study, C2C12 cells at 90% confluence were cultured for six days in differentiation medium. TGFβ (20ng/ml), E2 (10^{-6}M) or toremifene (10^{-6}M) alone or their combinations were added in the first three days only, or for all six days. To observe maximum effects of E2 on myotube formation, we further modified the growth condition. In the modified protocol, C2C12 cells at 90% confluence were cultured for three days in differentiation medium, then switched to estradiol-free differentiation medium (phenol-red free high glucose DMEM with 2% dextran-charcoal-stripped horse serum and 1% penicillin/streptomycin) with added TGFβ (20ng/ml), E2 (10^{-6}M) or toremifene (10^{-6}M) alone or their combinations for further three days.

Bindings of ERα to miR-486 regulatory region.

We used previously described ERα ChIP-seq data set generated using mouse mammary gland (24) to determine ERα binding sites in the regulatory region of *miR-486* as well as *Ank1* gene body where *miR-486* gene is located. DNA sequence spanning mouse chr.8: 23,139,501-23,141,502, which encompasses ERα binding site as per ChIP-seq and site is closest to *sANK1/miR-486* gene, was downloaded using UCSC Genome browser and five sets of primers were designed for qPCR. ChIP 1, Forward: 5'-GGA CTT AGG ATG TCT GCT CTT ATT-3'; Reverse: 5'-CCA GAG AAG TAA GGG AGA GAA TG-3'. ChIP 2,

Forward: 5'-CTG GGT CTT TCC CTT CTT CTA AC-3'; Reverse: 5'-GGC TCT GCT CTT ACC TTC TTG-3'. ChIP 3, Forward: 5'-CCT CTG GGT CCT CTA CAA TCT-3'; Reverse: 5'-GAC TAG GGC TGT GTG TTT CAT-3'. ChIP 4, forward: 5'-GTT CAC CTC CCA TTC TGG ATA AA-3'; Reverse: 5'-TCT GAC TAT CGT GCC TCT ACA-3'. ChIP 5, Forward: 5'-GGG ATC TGG AAG CAG ATA TTG AG-3'; Reverse: 5'-GCA ACC TGG AGC AAA GTA GA-3'. ChIP assay for ERα has been described previously (25). ChIP quality ERα antibody was from Santa Cruz Biotechnology (RRID:AB_631470 (26); Santa Cruz, CA, Cat# sc-542). DNA amplification CT values with IgG control antibody immunoprecipitation was normalized to one and relative amplification of DNA from ERα antibody immunoprecipitate under vehicle or E2 treatment for one hour was calculated. We selected this time point for E2 treatment because previous studies have shown maximum ERα binding to the genome 45-60 minutes after E2 treatment in breast cancer cells (25).

Total RNA extraction.

Total RNA isolation from skeletal muscle and C2C12 cells has been described previously (17,20).

Quantitative reverse transcription PCR (qRT-PCR).

Taqman miRNA Reverse Transcription kit (Applied Biosystems, #4366597) was used to synthesize cDNAs with 5µl of miRNAs (20-200 ng/µl) extracted from plasma, mouse muscle or C2C12 cells. Bio-RAD iScript cDNA synthesis kit (#170-8891) was used to reverse transcribe total RNAs (50-200 ng/µl) extracted from C2C12 cells to synthesize cDNAs in a final volume of 20 µL. qRT-PCR was performed using Taqman universal PCR master mix (Applied Biosystems, #4324018) and specific primers as described in our previous study (17,27). miR-16, U6 small RNA, and miR-30d were used as normalization controls for plasma, mouse muscle, and C2C12 cell microRNAs, respectively. Hsp90ab was

used as a normalization control for *Ank1* (Taqman Cat# Mm00482889) and *Srf* (Taqman Cat#Mm00491032) mRNA measurements in C2C12 cells.

Western blotting.

Harvested C2C12 cells were lysed in RIPA buffer with protease/phosphatase inhibitors (CST, Cat#5872S). Thirty micrograms of proteins were used for western blotting. Primary antibodies against SMAD2/3 (RRID:AB_10698742 (28); Cell Signaling Technology (CST) Cat#3102S, rabbit), p-SMAD2/3 (RRID:AB_2631089 (29); S465/467; CST, Cat#8828S, rabbit), p-SMAD1/5 (RRID:AB_491015 (30);S463/465, CST, Cat#9516, rabbit), SMAD1 (RRID:AB_2107780 (31); CST Cat#9743S, rabbit), PTEN (RRID:AB_2253290 (32); CST, Cat#9188, rabbit), p-AKT (RRID:AB_2315049 (33); S473, CST, Cat#4060, rabbit) and AKT (RRID:AB_915783 (34); CST, Cat#4691, rabbit) were used for western blots. Secondary antibody used for western blots was Anti-rabbit IgG, HRP-linked antibody (RRID:AB_2099233 (35); CST, Cat#7074). Quantification of western blotting was performed using NIH image J software.

Imaging analysis.

C2C12 myoblast cells (~10^4 cells/ well) were seeded in six well plates. After six days of differentiation with or without treatments, bright field images were captured with Keyence Microscope BZ-x810. Cells were washed three times with PBS for two minutes each, fixed in 4% PFA for 10 minutes, and rinsed three times with PBS. Fixed cells were blocked and permeabilized with blocking buffer (5% goat serum and 0.1% triton-X-100 in PBS) for one hour at room temperature. After rinsing with PBS, fixed cells were incubated with MF-20 (RRID:AB_2147781 (36); Myosin Heavy Chain, DSHB, 1:500 dilution) primary antibody solution containing 5% goat serum and 0.1% triton-X-100 in PBS overnight. Next day, cells were rinsed with PBS three times and incubated with secondary antibody (RRID:AB_142495

(37); Invitrogen, rabbit anti-mouse IgG conjugated with Alexa fluor 488, 1:1000) solution for one hour and rinsed with PBS three times. Stained cells were further incubated with 1:5000 Hoechst 33342 diluted in PBS for 10 minutes and rinsed with PBS three times. Finally, one ml PBS was added to each well. Images were acquired with Keyence Microscope BZ-x810. Cell count and measurement were processed with Keyence imaging analysis software.

Statistical analysis.

Data were analyzed using one-way ANOVA with Tukey's multiple comparisons test. A *P* value of <0.05 was considered statistically significant.

Results

Sex differences in cancer-induced loss of circulating miR-486.

Circulating microRNAs have been used as biomarkers to predict progression of cancers (38,39). We are interested in determining the levels of skeletal muscle-enriched miR-486 and inflammation-specific miR-146a in the circulating system as both have been reported to be potential biomarkers for cancer-associated systemic effects (20,40-42). We extracted total microRNAs from plasma of cancer patients and quantified microRNAs with qRT-PCR. CT values are presented as box plots in Fig. 1A. miR-486 and miR-146a levels in circulating system among patients with lung cancer, pancreatic cancer, and bladder cancer were normalized to miR-16 using the $2^{-\Delta\Delta Ct}$ method (21) and then converted into fold changes. When sex of patients was not taken into consideration, circulating miR-486 levels did not show significant changes in the plasma of lung and bladder cancer patients compared to healthy controls, although a significant decrease of miR-486 was observed in the plasma of

pancreatic cancer patients (Fig. 1B). However, a significant decrease of miR-146a levels was observed in the plasma of lung, pancreatic and bladder cancer patients compared to the plasma from healthy individuals (Fig. 1B).

A recent study identified sex-biased expression of miRNA genes, which are distributed across different chromosomes and chromosome 8 with *ANK1/miR-486* genes harbored several of these microRNAs (43). These observations along with the rationale described in the introduction section prompted us to re-analyze data taking sex of patients into consideration. Indeed, we observed significant decrease in circulating miR-486 in men but not in women with lung, pancreatic or bladder cancer (Fig. 1C and 1D), despite relatively small sample size. Cancer-induced reduction in circulating miR-146a was not influenced by sex of patients, at least in pancreatic and bladder cancer cases, suggesting some level of specificity in the effects of patient's sex on circulating microRNAs.

Male compared to female mice with orthotopic pancreatic cancer show lower circulating and skeletal muscle miR-486.

To further confirm sex-specific effects of cancer on miR-486 levels and the above observations are not biased due to small sample size, we implemented syngeneic pancreatic cancer model in mouse, and measured miR-486 and miR-146a levels in plasma and skeletal muscles. This acute compared to chronic models is ideal to discern the effects of sex on cancer-induced changes as our previous studies in chronic mammary tumor models have shown loss of circulating and skeletal muscle miR-486 in mammary tumor bearing female mice compared to control female mice (17,20,27). We found that male but not female mice with pancreatic cancer contained lower levels of circulating miR-486 (Fig. 2A). Since skeletal muscles are the major sources of miR-486 secreted into the circulating system (10), we next examined the levels of miR-486 in the skeletal muscle. Skeletal muscles of male but

not female mice contained lower levels of miR-486 compared to sex-matched control mice (Fig. 2B). Interestingly, both circulating and skeletal muscle miR-146a were not different in pancreatic cancer containing mice compared to control male and female mice (Fig. 2A and 2B). Thus, miR-486 is a specific marker of cancer-induced skeletal muscle defects, which is further influenced by the sex of patients.

E2 increases circulating miR-486 levels in male mice.

Since *miR-486* gene is located on chromosome 8 in both human and mouse but not in X-chromosome, the above noted sex-specific effect of cancer on circulating and skeletal muscle miR-486 levels is not a direct chromosomal effect. Female sex hormones are the likely candidates and we focused on E2 because of its known role in skeletal muscle. We implanted E2 pellet into male mice and examined the levels of circulating miR-486. Indeed, exogenous E2 significantly elevated circulating miR-486 levels in male mice (Fig. 2C). There was a modest increase in skeletal muscle miR-486 in E2 treated male mice, which did not reach statistical significance. It is possible that E2 increases miR-486 expression in skeletal muscle, but induced microRNA is released into circulation. Nonetheless, these results indicate the role of E2 on miR-486 expression.

miR-486 is an E2-regulated microRNA.

To understand the underlying mechanisms of E2 action on miR-486 levels, we used C2C12 myoblasts and their differentiated counterparts, which express Estrogen Receptor alpha (ERα) and Estrogen Receptor beta (ERβ) (44,45), to directly measure the effects of E2 on miR-486 expression. To increase translational potential of the study, we included the SERM toremifene, which shows central anti-estrogenic effect but estrogenic activity in liver (46). Toremifene has already been approved by FDA to prevent bone fractures in men with prostate cancer on androgen deprivation therapy (47). In undifferentiated myoblasts, E2

increased miR-486 with peak induction after 6 hours of E2 treatment (Fig. 3A and B). Toremifene also increased miR-486 suggesting that this SERM has estrogenic action in myoblasts (Fig. 3C).

The *miR-486* gene is located within a small *Ankyrin*-1 (*sANK1)* gene and is regulated by an alternative promoter immediately upstream of exon 39a of *ANK1* (10,48). miR-486 and sANK1 are co-expressed and co-regulated in muscle cells *in vitro* and skeletal muscles *in vivo* (10,20). Therefore, we further tested whether E2 and toremifene affect the expression of *sAnk1* and found that *sAnk1* is an E2 and toremifene-inducible gene (Fig. 3D). These results are consistent with the observation that E2 upregulates *Ank1* gene in animals (49). It has been reported that the Serum Response Factor (SRF) directly controls the transcription of *miR-486* gene (10). However, whether E2 and toremifene affect *Srf* gene expression is unknown. Here, we found that both E2 and toremifene promoted the expression of *Srf* mRNA in C2C12 myoblasts, SRF could be indirectly responsible for miR-486 induction by E2 and toremifene (Fig. 3D).

Differentiated myotubes express higher levels of miR-486 and expression of miR-486 in these cells is essential to maintain differentiated state (10,14). To determine whether E2 and toremifene regulate miR-486 expression in myotubes, we differentiated C2C12 cells (Fig. 3E) and examined the effects of E2 and toremifene on miR-486 expression. Both E2 and toremifene significantly increased miR-486 expression in myotubes (Fig. 3F), indicating E2 and toremifene are effective in increasing miR-486 in both C2C12 myoblasts and differentiated myotubes. Thus, previously reported E2-mediated myoblast differentiation is likely through miR-486 (11,16,50,51).

ERα binds directly to the regulatory regions of miR-486.

We used three approaches to determine whether ERα:E2 directly regulates miR-486. First, we explored ENCODE database (52) to identify transcription factors that may bind to regulatory region of human *miR-486/sANK1*. A binding site for ERα was observed in the regulatory region along with binding site for the pioneer factor FOXA1, which facilitates ERα binding to the genome (Fig. 4A) (53). Next, we used ERα ChIP-seq data of the mouse mammary gland to identify ERα binding sites in the regulatory regions of the mouse *miR-486*. Indeed, an ERα binding site was detected ~28 kB away from *miR-486* gene (Fig. 4B). Through ChIP-PCR for ERα, we verified bindings of ERα to this regulatory region. One binding site likely located within 114 bases surrounding chr8:23,139,734 (ChIP-1, Fig. 4C), the other binding site likely located within 107 bases surrounding chr8:23,140,390 (ChIP-3, Fig. 4D). Thus, it is likely that ERα directly regulates miR-486 expression.

E2 and toremifene reverse myostatin, TNFα and TGFβ-mediated inhibition of miR-486 expression.

We and others have previously shown that cytokines TNFα and TGFβ inhibit miR-486 expression and these two cytokines could be primary mediators of cancer-induced loss of miR-486 expression in skeletal muscle (20,54,55). Myostatin is another cytokine associated with muscle wasting in cancer (56-58). In C2C12 cells, myostatin reduces miR-486 and myostatin knockout mice express higher levels of miR-486 (59) and this reduction in miR-486 by myostatin requires activin receptor-like kinase (ALK) mediated phosphorylation of transcription factors SMAD2/3 (60). We examined whether E2 and toremifene can overcome the inhibitory effects of myostatin, TNFα and TGFβ on miR-486 expression in C2C12 cells. C2C12 cells were pretreated with E2, toremifene or vehicle for one hour followed by five hours treatment with TNFα or TGFβ. Cells were harvested for miR-486 analysis. Consistent

with the literature, myostatin, TNFα and TGFβ reduced miR-486 expression in both undifferentiated and differentiated C2C12 cells (Fig. 5A-C). However, in E2 or toremifene pre-treated undifferentiated and differentiated C2C12 cells, myostatin, TNFα and TGFβ failed to reduce miR-486 levels (Fig. 5A-C). Thus, E2 and toremifene can reverse the effects of cancer-induced cytokines on miR-486 expression.

E2 and toremifene antagonize myostatin-mediated SMAD2/3 activation.

Based on the literature, it is likely that TGFβ or myostatin activates ALK, which then phosphorylates SMAD2/3 to orchestrate *miR-486* gene repression (61,62). We examined whether E2 alters myostatin-mediated activation of SMAD2/3, which could potentially be a mechanism responsible for reversing the effects of myostatin on miR-486 expression. C2C12 cells were pretreated with E2 and toremifene for six hours, then myostatin was added to culture medium for 15 minutes. Cells were harvested for western blot analysis. We found that myostatin enhanced SMAD2/3 phosphorylation significantly in both undifferentiated and differentiated C2C12 cells (Fig. 5D and E). Pretreatment with E2 and toremifene greatly reduced SMAD2/3 phosphorylation levels in myostatin treated cells without altering the levels of total SMAD2/3 (Fig. 5D-F). Interestingly, E2 or toremifene did not alter myostatin-induced SMAD1/5 phosphorylation or total SMAD1 (Fig. 5G and H). Thus, E2 and toremifene specifically inhibit myostatin-induced SMAD2/3 activation.

E2 activates AKT in C2C12 cells.

Previous studies have demonstrated that miR-486 increases AKT signaling in skeletal muscles by negatively regulating PTEN (10,14,63). Recent study has shown that miR-486 expression is required to maintain AKT activation in C2C12 myoblasts (59). It has been postulated that cytokines such as myostatin activate SMAD2/3, which inhibits AKT signaling in skeletal muscle (61). Since E2 and toremifene increased miR-486, we next examined

whether these agents demonstrate beneficial effects on skeletal muscle by increasing phospho-AKT levels. C2C12 cells were treated for six hours with E2, toremifene or their combination, then harvested for western blotting. Indeed, both E2 and toremifene increased levels of both phosphorylated and total AKT1 (Fig. 6A, B and C) in both undifferentiated and differentiated C2C12 cells. As expected, both E2 and toremifene reduced the levels of PTEN in both undifferentiated and differentiated C2C12 cells (Fig. 6A, 6D). These results suggest the existence of ERα:E2-miR-486-AKT signaling network in skeletal muscle which can ward off deleterious effects of cytokines/chemokines and thus help to maintain muscle mass (13,64,65).

E2 and toremifene overcome TGFβ-mediated inhibition of myotube formation.

Recent studies have shown that TGFβ inhibits myoblast contacts *in vitro* and prevents muscle regeneration *in vivo* by modulating cell fusion (66,67). Whether E2 and toremifene have the ability to overcome TGFβ inhibition on muscle regeneration remains unknown. Since we observed the ability of E2 and toremifene to overcome the effects of TGFβ on miR-486 expression (Fig. 5B, C), we next examined whether E2 and toremifene can overcome the deleterious effects of TGFβ on myotube formation. C2C12 myoblasts were treated with recombinant TGFβ chronically for six days in 2% horse serum containing differentiation medium with vehicle, E2 or toremifene. Without TGFβ addition, C2C12 myoblasts fused into elongated myotubes under this growth condition. However, in the presence of TGFβ, size of myotubes was shorter (Fig. 7A, left column). These results were further confirmed by immunofluorescence staining of myosin heavy chain (MHC) protein (Fig. 7A., right column). These data indicate that TGFβ inhibits myotube formation, which is consistent with recent reports of TGFβ inhibiting myoblast fusion (66,67). E2 and toremifene treatment partially reversed the effects of TGFβ, as myotubes in TGFβ+E2 or

TGFβ+toremifene treated conditions were longer than under TGFβ alone treated condition but still remained thinner than under vehicle treated condition (Fig. 7A, right column). The diameters of differentiated myotubes were 44±1.9 μm, 46±2.2 μm, 44±1.8 μm, 15±1.1 μm, 29±2 μm, and 28±1.5 μm, respectively, in vehicle, E2, toremifene, TGFβ, TGFβ/E2 and TGFβ/toremifene treated group.

We next determined whether the effects of TGFβ on myotube is reversible and E2 or toremifene accelerates this reversal. C2C12 myoblasts were treated with TGFβ for 3 days in 2% horse serum containing differentiation medium with vehicle, E2 or toremifene and then switched to differentiation medium without TGFβ, E2 or toremifene for further 3 days for full differentiation. We found that C2C12 myoblasts had converted into well-developed myotubes even under 3 days of TGFβ treatment followed by TGFβ withdrawal, although the size of myotubes were still smaller than vehicle control group (Fig. 7B). E2 or toremifene co-treatments greatly improved myotube size and branching compared to conditions with TGFβ treatment alone (Fig. 7B). The diameters of differentiated myotubes were 46±2.1 μm, 46±1.5 μm, 44±1.7 μm, 24±1.1 μm, 35±1.4 μm, and 36±1.7 μm, respectively, in vehicle, E2, toremifene, TGFβ, TGFβ/E2, and TGFβ/toremifene treated group. These data indicate that the effects of TGFβ on muscle regeneration *in vitro* are reversible and E2 or toremifene can accelerate this recovery.

Considering that regular medium has phenol red, which has weak estrogen-like effects (68), and regular serum contains significant levels of E2 to activate ERα, we modified growth conditions to document maximum effects of E2 on myotube formation. C2C12 myoblasts were grown in regular differentiation medium (Phenol red containing medium with 2% normal horse serum) for three days, then switched to phenol red free differentiation medium with 2% dextran-charcoal-stripped horse serum for further three days differentiation. Prolonged

maintenance in this medium was deleterious to cells. TGFβ, E2, toremifene or their combinations were added after three days of culturing in regular differentiation medium. MHC immunofluorescent analysis revealed that vehicle, E2 or toremifene treated C2C12 myoblasts differentiated into well-developed myotubes (Fig. 7C, right column). However, TGFβ treatment alone greatly reduced the size and length of myotubes. Longer myotubes were observed in E2/TGFβ and toremifene/TGFβ treated C2C12 cells compared to TGFβ treatment alone (Fig. 7C, right column). The lengths of differentiated C2C12 myotubes were 491±61 μm, 497±74 μm, 460±47 μm, 288±42 μm, 469±63 μm, and 434±50 μm, respectively, in vehicle, E2, toremifene, TGFβ, TGFβ/E2 and TGFβ/toremifene treated group. The diameters of differentiated myotubes were 41±2.1 μm, 43±1.9 μm, 45±2.0 μm, 38±1.8 μm, 43±1.9 μm, and 44±2.5 μm, respectively, in vehicle, E2, toremifene, TGFβ, TGFβ/E2 and TGFβ/toremifene treated group. These results indicate that TGFβ inhibits myoblasts to myotube differentiation and E2 or toremifene can reverse the negative effect of TGFβ on myogenic differentiation.

Discussion

Altered cytokine levels derived from host immune cells in response to tumors and/or by the tumor itself contribute to functional limitations and muscle wasting with eventual clinical manifestation as cachexia (69,70). High plasma levels of TNFα and TGFβ have been observed in both tumor-bearing animals and cachectic cancer patients (17,20,71,72). TGFβ and its family members contribute to muscle wasting by activating SMAD2/3 via ALK (61,62). A primary target of SMAD2/3 is AKT, which is a critical signaling node in skeletal muscle (73). Activated AKT contributes to myogenesis and muscle mass homeostasis (10). Skeletal muscle enriched miR-486 maintains active AKT levels by downregulating PTEN. Therefore, it is not surprising that cancer-induced skeletal muscle wasting involves loss of miR-486 expression (Fig. 8, left panel). Studies by multiple groups including us demonstrated a role for cancer-induced cytokines in reducing skeletal muscle miR-486 (20). In our search to identify agents that can reverse cancer-induced loss of skeletal muscle miR-486, we had previously reported the ability of the NF-κB inhibitor dimethylaminoparthenolide in reversing cancer-induced loss of miR-486 and restoring skeletal muscle function (17,27). In present study, we report two other agents, one natural and one synthetic, for their ability to increase miR-486 levels in skeletal muscle and potentially overcome the deleterious effects of cancer on skeletal muscle as shown schematically in Fig. 8. Levels of cancer-induced TNFα and TGFβ1 and physiologic levels of E2, which can be affected by menopausal status or chemotherapy treatment for cancer, ultimately determine degree of cancer-induced changes in myogenesis (51). In our model system, E2 and toremifene could not completely reverse the actions of cytokines on miR-486 expression (Fig. 5). This could be due to convergence of multiple cytokine-activated signaling pathways on *miR-486/sANK1* regulatory regions and E2 and toremifene may antagonize few but not all of these signaling pathways.

Identification of E2 as an agent that can increase miR-486 levels provides an explanation as to why cancer-induced skeletal muscle defects are much more severe in men compared to women. Although E2 therapy for men with cancer may have side effects such as feminization, toremifene with similar activity on miR-486 expression but tissue specific ERα agonistic and antagonistic activities and lower side effects than E2, can be used to reduce cancer-associated skeletal muscle defects.

There are at least three potential mechanisms by which E2 can regulate miR-486 expression (Fig. 8). ERα:E2 can bind directly to the regulatory region of *miR-486/sANK1* gene as shown in Fig. 4. Since toremifene could also increase miR-486, it is likely that this agent functions as an agonist in skeletal muscle cells and utilizes ERα to activate miR-486 expression. We also observed *SRF* as an E2-inducible gene, which is required for miR-486 expression. The third possibility is through inhibition of NF-κB. Cancer-induced cytokines are suggested to inhibit miR-486 by activating NF-κB and we had previously reported the ability of ERα:E2 to repress NF-κB activity (74). Therefore, E2 can induce miR-486 through multiple mechanisms (Fig. 8).

E2 or toremifene treatment increased phospho-AKT levels with corresponding decrease in PTEN levels. We also found elevated levels of total AKT1 in E2 and toremifene-treated cells, which could be an indirect consequence of phosphorylation mediated stabilization of AKT or E2 directly inducing AKT1 expression, which consequently increases phospho-AKT levels. Although less is known about E2:ERα directly regulating AKT1 in human cells, AKT1 in hens is directly regulated by E2:ERα (75). Depending on cell types, E2 may increase phospho-AKT levels through rapid non-genomic action (76,77). However, time course studies exclude such a possibility. We favor the possibility that in addition to direct AKT1 regulation, E2 or toremifene increases miR-486, which leads to elevated

phospho-AKT because of lower PTEN levels. Although overexpression studies with anti-mer to miR-486 can examine this hypothesis, we found manipulating miR-486 levels through both anti-mers and overexpression in C2C12 cells to be extremely difficult. Whatever the mechanism of E2-mediated upregulation of miR-486 is, our results have important implications on how cancer-induced skeletal muscle wasting can be managed. Chemotherapy typically causes ovarian dysfunction and ovarian suppression is actively pursued to reduce recurrence in premenopausal breast cancer patients (78). Thus, E2 levels in premenopausal women undergoing cancer treatment could be similar to levels in men and these women could potentially face devastating skeletal muscle dysfunction similar to men. Toremifene, which has shown strong safety profile in clinical trials could be used in these women to overcome treatment-induced skeletal muscle defects (79). Collectively, our studies reveal miR-486 as a sex-specific functional biomarker of cancer-induced systemic effects and its levels can be therapeutically manipulated with existing agents to improve outcome in cancer patients.

Acknowledgements: We thank Mr. Tim Breen of HCRN and Komen Normal Tissue Bank for providing human plasma samples and Ms. Duojiao Chen for aligning mouse mammary gland ERα ChIP-seq data to regulatory regions of *miR-486* and *sANK1* regulatory regions.

Author Contribution: RW, experimental design and execution, data collection and analyses, and manuscript writing; PBN, Lab technical support; XZ, TZ, support in pancreatic cancer model; HN, study supervision, experimental design, data interpretation and manuscript writing.

References:

1. Norman K, Stobaus N, Reiss J, Schulzke J, Valentini L, Pirlich M. Effect of sexual dimorphism on muscle strength in cachexia. *J Cachexia Sarcopenia Muscle*. 2012;3(2):111-116.
2. Zhong X, Zimmers TA. Sex Differences in Cancer Cachexia. *Curr Osteoporos Rep*. 2020.
3. Ventetuolo CE, Hess E, Austin ED, Baron AE, Klinger JR, Lahm T, Maddox TM, Plomondon ME, Thompson L, Zamanian RT, Choudhary G, Maron BA. Sex-based differences in veterans with pulmonary hypertension: Results from the veterans affairs-clinical assessment reporting and tracking database. *PloS one*. 2017;12(11):e0187734.
4. Ikeda K, Horie-Inoue K, Inoue S. Functions of estrogen and estrogen receptor signaling on skeletal muscle. *J Steroid Biochem Mol Biol*. 2019;191:105375.
5. Ikeda Y, Kato-Inui T, Tagami A, Maekawa M. Expression of progesterone receptor, estrogen receptors alpha and beta, and kisspeptin in the hypothalamus during perinatal development of gonad-lacking steroidogenic factor-1 knockout mice. *Brain Res*. 2019;1712:167-179.
6. Takahashi T, Iwasaki A. Sex differences in immune responses. *Science*. 2021;371(6527):347-348.
7. Priego T, Martin AI, Gonzalez-Hedstrom D, Granado M, Lopez-Calderon A, Cardalini D. Role of hormones in sarcopenia. *Vitam Horm*. 2021;115:535-570.
8. Torres J, Palmela C, Gomes de Sena P, Santos MPC, Gouveia C, Oliveira MH, Henriques AR, Rodrigues C, Cravo M, Borralho P. Farnesoid X Receptor Expression in Microscopic Colitis: A Potential Role in Disease Etiopathogenesis. *GE Port J Gastroenterol*. 2018;25(1):30-37.
9. Enns DL, Tiidus PM. The influence of estrogen on skeletal muscle: sex matters. *Sports Med*. 2010;40(1):41-58.
10. Small EM, O'Rourke JR, Moresi V, Sutherland LB, McAnally J, Gerard RD, Richardson JA, Olson EN. Regulation of PI3-kinase/Akt signaling by muscle-enriched microRNA-486. *Proc Natl Acad Sci U S A*. 2010;107(9):4218-4223.
11. Holstein I, Singh AK, Pohl F, Misiak D, Braun J, Leitner L, Huttelmaier S, Posern G. Post-transcriptional regulation of MRTF-A by miRNAs during myogenic differentiation of myoblasts. *Nucleic Acids Res*. 2020;48(16):8927-8942.
12. Chacon-Cabrera A, Gea J, Barreiro E. Short- and Long-Term Hindlimb Immobilization and Reloading: Profile of Epigenetic Events in Gastrocnemius. *J Cell Physiol*. 2017;232(6):1415-1427.
13. Alexander MS, Casar JC, Motohashi N, Myers JA, Eisenberg I, Gonzalez RT, Estrella EA, Kang PB, Kawahara G, Kunkel LM. Regulation of DMD pathology by an ankyrin-encoded miRNA. *Skeletal muscle*. 2011;1:27.
14. Alexander MS, Casar JC, Motohashi N, Vieira NM, Eisenberg I, Marshall JL, Gasperini MJ, Lek A, Myers JA, Estrella EA, Kang PB, Shapiro F, Rahimov F, Kawahara G, Widrick JJ, Kunkel LM. MicroRNA-486-dependent modulation of DOCK3/PTEN/AKT signaling pathways improves muscular dystrophy-associated symptoms. *J Clin Invest*. 2014;124(6):2651-2667.
15. Rylie M. Hightower eS, Andrea L. Reid, Katherine G. English, et al. miR-486 is an epigenetic modulator of Duchenne muscular dystrophy pathologies. *BioRxiv*. 2021.
16. Dey BK, Gagan J, Dutta A. miR-206 and -486 induce myoblast differentiation by downregulating Pax7. *Mol Cell Biol*. 2011;31(1):203-214.
17. Wang R, Bhat-Nakshatri P, Padua MB, Prasad MS, Anjanappa M, Jacobson M, Finnearty C, Sefcsik V, McElyea K, Redmond R, Sandusky GE, Penthala N, Crooks PA, Liu J, Zimmers T, Nakshatri H. Pharmacological dual inhibition of tumor and tumor-induced functional limitations in transgenic model of breast cancer. *Mol Cancer Ther*. 2017:2747-2758.
18. Wang R, Kumar B, Bhat-Nakshatri P, Prasad MS, Jacobsen MH, Ovalle G, Maguire C, Sandusky G, Trivedi T, Mohammad KS, Guise T, Penthala NR, Crooks PA, Liu J, Zimmers T, Nakshatri H. Aging-associated skeletal muscle defects in HER2/Neu transgenic mammary tumor model. *JCSM Rapid Commun*. 2021;4(1):24-39.

19. Hakim CH, Duan D. Gender differences in contractile and passive properties of mdx extensor digitorum longus muscle. *Muscle Nerve*. 2012;45(2):250-256.
20. Chen D, Goswami CP, Burnett RM, Anjanappa M, Bhat-Nakshatri P, Muller W, Nakshatri H. Cancer Affects microRNA Expression, Release, and Function in Cardiac and Skeletal Muscle. *Cancer Res*. 2014;74:4270-4281.
21. Beg F, Wang R, Saeed Z, Devaraj S, Masoor K, Nakshatri H. Inflammation-associated microRNA changes in circulating exosomes of heart failure patients. *BMC Res Notes*. 2017;10(1):751.
22. Hingorani SR, Wang L, Multani AS, Combs C, Deramaudt TB, Hruban RH, Rustgi AK, Chang S, Tuveson DA. Trp53R172H and KrasG12D cooperate to promote chromosomal instability and widely metastatic pancreatic ductal adenocarcinoma in mice. *Cancer Cell*. 2005;7(5):469-483.
23. Zhong X, Pons M, Poirier C, Jiang Y, Liu J, Sandusky GE, Shahda S, Nakeeb A, Schmidt CM, House MG, Ceppa EP, Zyromski NJ, Liu Y, Jiang G, Couch ME, Koniaris LG, Zimmers TA. The systemic activin response to pancreatic cancer: implications for effective cancer cachexia therapy. *J Cachexia Sarcopenia Muscle*. 2019;10(5):1083-1101.
24. Palaniappan M, Nguyen L, Grimm SL, Xi Y, Xia Z, Li W, Coarfa C. The genomic landscape of estrogen receptor alpha binding sites in mouse mammary gland. *PLoS One*. 2019;14(8):e0220311.
25. Bhat-Nakshatri P, Wang G, Appaiah H, Luktuke N, Carroll JS, Geistlinger TR, Brown M, Badve S, Liu Y, Nakshatri H. AKT alters genome-wide estrogen receptor alpha binding and impacts estrogen signaling in breast cancer. *Mol Cell Biol*. 2008;28(24):7487-7503.
26. RRID:AB_631470.
27. Ruizhong Wang BK, Poornima Bhat-Nakshatri , Mayuri S Prasad , Max H Jacobsen , Gabriela Ovalle , Calli Maguire , George Sandusky , Trupti Trivedi , Khalid S Mohammad , Theresa Guise , Narsimha R Penthala , Peter A Crooks , Jianguo Liu , Teresa Zimmers , Harikrishna Nakshatri Aging-associated skeletal muscle defects in HER2/Neu transgenic mammary tumor model. *Journal of Cachexia, Sarcopenia and Muscle Rapid Communications*. 2021;4(1):24-39.
28. RRID:AB_10698742.
29. RRID:AB_2631089.
30. RRID:AB_491015.
31. RRID:AB_2107780.
32. RRID:AB_2253290.
33. RRID:AB_2315049.
34. RRID:AB_915783.
35. RRID:AB_2099233.
36. RRID:AB_2147781.
37. RRID:AB_142495.
38. Backes C, Meese E, Keller A. Specific miRNA Disease Biomarkers in Blood, Serum and Plasma: Challenges and Prospects. *Mol Diagn Ther*. 2016;20(6):509-518.
39. Cui W, Ma J, Wang Y, Biswal S. Plasma miRNA as biomarkers for assessment of total-body radiation exposure dosimetry. *PLoS One*. 2011;6(8):e22988.
40. Li C, Zheng X, Li W, Bai F, Lyu J, Meng QH. Serum miR-486-5p as a diagnostic marker in cervical cancer: with investigation of potential mechanisms. *BMC Cancer*. 2018;18(1):61.
41. Tian F, Shen Y, Chen Z, Li R, Lu J, Ge Q. Aberrant miR-181b-5p and miR-486-5p expression in serum and tissue of non-small cell lung cancer. *Gene*. 2016;591(2):338-343.
42. Sromek M, Glogowski M, Chechlinska M, Kulinczak M, Szafron L, Zakrzewska K, Owczarek J, Wisniewski P, Wlodarczyk R, Talarek L, Turski M, Siwicki JK. Changes in plasma miR-9, miR-16, miR-205 and miR-486 levels after non-small cell lung cancer resection. *Cell Oncol (Dordr)*. 2017;40(5):529-536.
43. Cui C, Yang W, Shi J, Zhou Y, Yang J, Cui Q, Zhou Y. Identification and Analysis of Human Sex-biased MicroRNAs. *Genomics Proteomics Bioinformatics*. 2018;16(3):200-211.
44. Milanesi L, Russo de Boland A, Boland R. Expression and localization of estrogen receptor alpha in the C2C12 murine skeletal muscle cell line. *J Cell Biochem*. 2008;104(4):1254-1273.

45. Milanesi L, Vasconsuelo A, de Boland AR, Boland R. Expression and subcellular distribution of native estrogen receptor beta in murine C2C12 cells and skeletal muscle tissue. *Steroids*. 2009;74(6):489-497.
46. Roelfsema F, Yang RJ, Takahashi PY, Erickson D, Bowers CY, Veldhuis JD. Effects of Toremifene, a Selective Estrogen Receptor Modulator, on Spontaneous and Stimulated GH Secretion, IGF-I, and IGF-Binding Proteins in Healthy Elderly Subjects. *J Endocr Soc*. 2018;2(2):154-165.
47. Poon Y, Pechlivanoglou P, Alibhai SMH, Naimark D, Hoch JS, Papadimitropoulos E, Hogan ME, Krahn M. Systematic review and network meta-analysis on the relative efficacy of osteoporotic medications: men with prostate cancer on continuous androgen-deprivation therapy to reduce risk of fragility fractures. *BJU Int*. 2018;121(1):17-28.
48. Oh HK, Tan AL, Das K, Ooi CH, Deng NT, Tan IB, Beillard E, Lee J, Ramnarayanan K, Rha SY, Palanisamy N, Voorhoeve PM, Tan P. Genomic loss of miR-486 regulates tumor progression and the OLFM4 antiapoptotic factor in gastric cancer. *Clin Cancer Res*. 2011;17(9):2657-2667.
49. Kim HJ, Gieske MC, Trudgen KL, Hudgins-Spivey S, Kim BG, Krust A, Chambon P, Jeong JW, Blalock E, Ko C. Identification of estradiol/ERalpha-regulated genes in the mouse pituitary. *J Endocrinol*. 2011;210(3):309-321.
50. Fochi S, Giuriato G, De Simone T, Gomez-Lira M, Tamburin S, Del Piccolo L, Schena F, Venturelli M, Romanelli MG. Regulation of microRNAs in Satellite Cell Renewal, Muscle Function, Sarcopenia and the Role of Exercise. *Int J Mol Sci*. 2020;21(18).
51. Galluzzo P, Rastelli C, Bulzomi P, Acconcia F, Pallottini V, Marino M. 17beta-Estradiol regulates the first steps of skeletal muscle cell differentiation via ER-alpha-mediated signals. *Am J Physiol Cell Physiol*. 2009;297(5):C1249-1262.
52. Davis CA, Hitz BC, Sloan CA, Chan ET, Davidson JM, Gabdank I, Hilton JA, Jain K, Baymuradov UK, Narayanan AK, Onate KC, Graham K, Miyasato SR, Dreszer TR, Strattan JS, Jolanki O, Tanaka FY, Cherry JM. The Encyclopedia of DNA elements (ENCODE): data portal update. *Nucleic Acids Res*. 2018;46(D1):D794-D801.
53. Zaret KS, Carroll JS. Pioneer transcription factors: establishing competence for gene expression. *Genes Dev*. 2011;25(21):2227-2241.
54. Argiles JM, Busquets S, Toledo M, Lopez-Soriano FJ. The role of cytokines in cancer cachexia. *Curr Opin Support Palliat Care*. 2009;3(4):263-268.
55. Wang R, Nakshatri H. Systemic Actions of Breast Cancer Facilitate Functional Limitations. *Cancers (Basel)*. 2020;12(1).
56. Lokireddy S, Wijesoma IW, Bonala S, Wei M, Sze SK, McFarlane C, Kambadur R, Sharma M. Myostatin is a novel tumoral factor that induces cancer cachexia. *Biochem J*. 2012;446(1):23-36.
57. Loumaye A, de Barsy M, Nachit M, Lause P, Frateur L, van Maanen A, Trefois P, Gruson D, Thissen JP. Role of Activin A and myostatin in human cancer cachexia. *J Clin Endocrinol Metab*. 2015;100(5):2030-2038.
58. Costelli P, Muscaritoli M, Bonetto A, Penna F, Reffo P, Bossola M, Bonelli G, Doglietto GB, Baccino FM, Rossi Fanelli F. Muscle myostatin signalling is enhanced in experimental cancer cachexia. *Eur J Clin Invest*. 2008;38(7):531-538.
59. Hitachi K, Nakatani M, Tsuchida K. Myostatin signaling regulates Akt activity via the regulation of miR-486 expression. *The international journal of biochemistry & cell biology*. 2014;47:93-103.
60. Graham ZA, De Gasperi R, Bauman WA, Cardozo CP. Recombinant myostatin reduces highly expressed microRNAs in differentiating C2C12 cells. *Biochem Biophys Rep*. 2017;9:273-280.
61. Rodriguez J, Vernus B, Chelh I, Cassar-Malek I, Gabillard JC, Hadj Sassi A, Seiliez I, Picard B, Bonnieu A. Myostatin and the skeletal muscle atrophy and hypertrophy signaling pathways. *Cell Mol Life Sci*. 2014;71(22):4361-4371.
62. Elkina Y, von Haehling S, Anker SD, Springer J. The role of myostatin in muscle wasting: an overview. *J Cachexia Sarcopenia Muscle*. 2011;2(3):143-151.

63. Hitachi K, Tsuchida K. Role of microRNAs in skeletal muscle hypertrophy. *Front Physiol*. 2013;4:408.
64. Quan-Jun Y, Yan H, Yong-Long H, Li-Li W, Jie L, Jin-Lu H, Jin L, Peng-Guo C, Run G, Cheng G. Selumetinib Attenuates Skeletal Muscle Wasting in Murine Cachexia Model through ERK Inhibition and AKT Activation. *Mol Cancer Ther*. 2017;16(2):334-343.
65. Talbert EE, Yang J, Mace TA, Farren MR, Farris AB, Young GS, Elnaggar O, Che Z, Timmers CD, Rajasekera P, Maskarinec JM, Bloomston M, Bekaii-Saab T, Guttridge DC, Lesinski GB. Dual Inhibition of MEK and PI3K/Akt Rescues Cancer Cachexia through both Tumor-Extrinsic and -Intrinsic Activities. *Mol Cancer Ther*. 2017;16(2):344-356.
66. Girardi F, Taleb A, Ebrahimi M, Datye A, Gamage DG, Peccate C, Giordani L, Millay DP, Gilbert PM, Cadot B, Le Grand F. TGFbeta signaling curbs cell fusion and muscle regeneration. *Nat Commun*. 2021;12(1):750.
67. Melendez J, Sieiro D, Salgado D, Morin V, Dejardin MJ, Zhou C, Mullen AC, Marcelle C. TGFbeta signalling acts as a molecular brake of myoblast fusion. *Nat Commun*. 2021;12(1):749.
68. Berthois Y, Katzenellenbogen JA, Katzenellenbogen BS. Phenol red in tissue culture media is a weak estrogen: implications concerning the study of estrogen-responsive cells in culture. *Proc Natl Acad Sci U S A*. 1986;83(8):2496-2500.
69. Argiles JM, Busquets S, Lopez-Soriano FJ. Cytokines in the pathogenesis of cancer cachexia. *Curr Opin Clin Nutr Metab Care*. 2003;6(4):401-406.
70. Fearon K, Arends J, Baracos V. Understanding the mechanisms and treatment options in cancer cachexia. *Nature reviews Clinical oncology*. 2013;10(2):90-99.
71. Tisdale MJ. Mechanisms of cancer cachexia. *Physiol Rev*. 2009;89(2):381-410.
72. Hogan KA, Cho DS, Arneson PC, Samani A, Palines P, Yang Y, Doles JD. Tumor-derived cytokines impair myogenesis and alter the skeletal muscle immune microenvironment. *Cytokine*. 2018;107:9-17.
73. Egerman MA, Glass DJ. Signaling pathways controlling skeletal muscle mass. *Crit Rev Biochem Mol Biol*. 2014;49(1):59-68.
74. Nakshatri H, Bhat-Nakshatri P, Martin DA, Goulet RJ, Jr., Sledge GW, Jr. Constitutive activation of NF-kappaB during progression of breast cancer to hormone-independent growth. *Mol Cell Biol*. 1997;17(7):3629-3639.
75. Guo M, Li Y, Chen Y, Guo X, Yuan Z, Jiang Y. Genome-wide mapping of estrogen receptor alpha binding sites by ChIP-seq to identify genes related to sexual maturity in hens. *Gene*. 2018;642:32-42.
76. Majumdar S, Rinaldi JC, Malhotra NR, Xie L, Hu DP, Gauntner TD, Grewal HS, Hu WY, Kim SH, Katzenellenbogen JA, Kasper S, Prins GS. Differential Actions of Estrogen Receptor alpha and beta via Nongenomic Signaling in Human Prostate Stem and Progenitor Cells. *Endocrinology*. 2019;160(11):2692-2708.
77. Kelly MJ, Levin ER. Rapid actions of plasma membrane estrogen receptors. *Trends Endocrinol Metab*. 2001;12(4):152-156.
78. Francis PA, Regan MM, Fleming GF, Lang I, Ciruelos E, Bellet M, Bonnefoi HR, Climent MA, Da Prada GA, Burstein HJ, Martino S, Davidson NE, Geyer CE, Jr., Walley BA, Coleman R, Kerbrat P, Buchholz S, Ingle JN, Winer EP, Rabaglio-Poretti M, Maibach R, Ruepp B, Giobbie-Hurder A, Price KN, Colleoni M, Viale G, Coates AS, Goldhirsch A, Gelber RD, Investigators S, International Breast Cancer Study G. Adjuvant ovarian suppression in premenopausal breast cancer. *N Engl J Med*. 2015;372(5):436-446.
79. Steiner MS, Pound CR. Phase IIA clinical trial to test the efficacy and safety of Toremifene in men with high-grade prostatic intraepithelial neoplasia. *Clin Prostate Cancer*. 2003;2(1):24-31.

Figure legends

Figure 1: Lower levels of circulating miR-486 in patients with different types of cancer. Total miRNAs were extracted from human plasma and amplified by qRT-PCR for miR-486 and miR-146a. **A.** Box plot shows distribution patterns of CT values. **B.** Analysis of miR-486 and miR-146a levels in human plasma. miR-16 was used as a normalization control. miR-486 was significantly downregulated in plasma of pancreatic cancer patients, but not in lung and bladder cancer patients compared to plasma of healthy donors. Circulating levels of miR-146a were lower in all cancer patients compared to healthy donors. **C.** Subset analysis of plasma from only women healthy donors and cancer patients. **D.** Subset analysis of plasma from only men healthy donors and cancer patients. Circulating miR-486 and miR-146a levels were lower in all men with cancer compared to healthy donors. * indicates significance between healthy group and cancer group (*$p<0.05$, **$p\leq0.005$, ***$p\leq0.0005$).

Figure 2: Reduced levels of miR-486 in plasma and skeletal muscles of mice with orthotopic KPC32908 cell line derived pancreatic cancer. **A.** Circulating miR-486 levels were significantly lower in male, but not in female, mice with pancreatic cancer compared to sex-matched healthy mice. miR-146a levels were unaffected. **B.** miR-486 was lower in quadriceps skeletal muscle of male, but not in female, mice compared to quadriceps of control mice. miR-146a was unaffected in both male and female mice. * indicates significance between healthy group and tumor cell implantation group (**$p\leq0.005$, ***$p\leq0.0005$). **C.** Healthy male mice implanted with E2 pellets show elevated circulating miR-486. Circulating levels of miR-486 was elevated in male mice implanted with E2 pellet compared to sham-treated age matched control mice (*$p=0.0156$). E2 had modest/non-significant effect on skeletal muscle miR-486, potentially due to release of miR-486 from skeletal muscle to circulation.

Figure 3: E2 increases miR-486 expression in C2C12 cells. **A.** Phase contrast image of undifferentiated C2C12 cells. **B.** Time course analysis of miR-486 expression in C2C12 myoblasts treated with E2 (n=6). **C.** Both E2 (10^{-10}M) and toremifene (10^{-6}M) induced miR-486 expression. **D.** mRNA levels of *Ank1* and *Srf* in C2C12 myoblasts six hours after treatment with E2 and toremifene. **E.** Phase contrast images of differentiated C2C12 cells. **F.** Both E2 and toremifene increased miR-486 expression in C2C12 myotubes six hours after treatment. * indicates significance between vehicle group and treated group (*$p<0.05$, **$p\leq0.005$, ***$p\leq0.0005$).

Figure 4: ERα binds directly to regulatory regions close to *miR-486/sANK1* gene. **A.** Schematic view of human *miR-486/sANK1* gene with potential transcription factor binding sites annotated using the ENCODE database. ERα binding site is indicated. **B.** ERα binding sites close to *miR-486/Ank1* gene in mouse. ERα ChIP-seq data from mouse mammary gland (GSE130032) with two replicates were used to identify ERα binding sites. **C.** Validation of ERα binding to regulatory region of *miR-486* in C2C12 cells using ChIP primer set 1 (n=5). **D.** Validation of ERα binding to regulatory region of *miR-486* in C2C12 cells using ChIP primer set 3 (n=5). ChIP-DNA enrichment in IgG control immunoprecipitates was normalized to one and relative differences in ERα ChIP with and without E2 treatment are shown. Two motifs within 2000 base long regulatory region showed ERα binding.

Figure 5: E2 (10^{-10}M) and toremifene (10^{-6}M) reversed inhibitory actions of myostatin (100ng/ml), TNFα (20ng/ml) and TGFβ (20ng/ml) on miR-486 expression. **A.** Undifferentiated C2C12 myoblasts and differentiated C2C12 myotubes were treated with vehicle, E2 or toremifene for one hour, then myostatin or vehicle was added to the culture medium for five hours (n=6). **B**. Undifferentiated C2C12 myoblasts and differentiated C2C12 myotubes were treated with vehicle or E2 for one hour, then TNFα, TGFβ or vehicle were

added to the culture medium for five hours (n=6). **C.** Undifferentiated C2C12 myoblasts and differentiated C2C12 myotubes were treated with vehicle or toremifene for one hour, then TNFα, TGFβ or vehicle were added to the culture medium for five hours (n=6). * indicates significance between vehicle group and treated group (**p≤0.005, ***p≤0.0005). **D**. E2 and toremifene reduce myostatin-induced phosphorylation of SMAD2/3, particularly in differentiated myotubes. Phospho-SMAD2/3 and SMAD2/3 blots are from two different gel electrophoresis but from the same batch of extracts. SMAD2/3 blot reprobed for βActin is shown. Phospho-SMAD1/5 and SMAD1/5 were also analyzed similarly. **E.** Quantitative analysis of SMAD2/3 phosphorylation by image J. **F.** Quantitative analysis of total SMAD2/3. **G.** Quantitative analysis of phospho-SMAD1/5 **H.** Quantitative analysis of total SMAD1. * indicates significance between vehicle group and treated group (*p<0.05, **p≤0.005; n=3). $^{\#}$ indicates significance between myostatin alone group and myostatin plus E2/or toremifene treated group ($^{\#}$p<0.05).

Figure 6: E2 induces AKT phosphorylation. **A**. Protein expression levels of AKT and PTEN in C2C12 cells with E2 and toremifene treatments. **B.** Quantitative analysis of phospho-AKT. **C.** Quantitative analysis total AKT1. **D.** Quantitative analysis of PTEN. * indicates significance between vehicle group and treated group (*p<0.05, **p≤0.005, ***p≤0.0005; n=3).

Figure 7: E2 and toremifene overcome inhibitory effects of TGFβ on myogenic differentiation and myotube formation. **A.** C2C12 cells were allowed to differentiate for six days in high glucose DMEM medium with 2% horse serum. The media were supplemented with vehicle, TGFβ (20ng/ml), E2 (10^{-6}M) or toremifene (10^{-6}M) alone, or their combinations for all six days. Bright field view (left column) and immunofluorescent labeling of myosin heavy chain in differentiated myotubes (right column). **B.** C2C12 cells were cultured six days

in high glucose DMEM medium with 2% horse serum, but TGFβ (20ng/ml), E2 (10^{-6}M) or toremifene (10^{-6}M) alone, or their combinations were applied only for the first three days in the culture media. Bright field views (left column) and immunofluorescent labeling of myosin heavy chain in differentiated myotubes (right column) are shown. **C.** C2C12 cells were cultured three days in high glucose DMEM medium with 2% horse serum, then switched to phenol red free high glucose DMEM medium with charcoal stripped 2% horse serum for further three days. Vehicle, TGFβ (20ng/ml), E2 (10^{-6}M) or toremifene (10^{-6}M) alone, or their combinations were added during subsequent three days in culture. Bright field views (left column) and immunofluorescent labeling of myosin heavy chain in differentiated myotubes (right column) are shown.

Figure 8: A model depicting ERα:E2:miR-486:AKT signaling axis in skeletal muscle and its sex-specific role in controlling cancer-induced skeletal muscle defects. (Left panel) In patients with cancer, tumors or host cells in response to tumors release cytokines and chemokines (e.g. myostatin, TNFα and TGFβ), which activate SMAD2/3 in skeletal muscle. Activated SMAD2/3 inhibits AKT activity, skeletal muscle protein synthesis and skeletal muscle function, which ultimately results in lower levels of miR-486 and delayed myogenic differentiation. (Right panel) In women with cancer, sex hormone E2 binds to ER and then directly or indirectly via SRF acts on *sANK1* gene transcription regulatory regions. As a consequence, transcripts levels of *sANK1* and *miR-486* are increased. miR-486 then induces AKT phosphorylation by reducing the levels of PTEN leading to enhanced skeletal muscle function, muscle mass and myogenesis. As a feed-forward loop, E2-mediated restoration of muscle functions may lead to further elevated levels of miR-486.

Figure 1

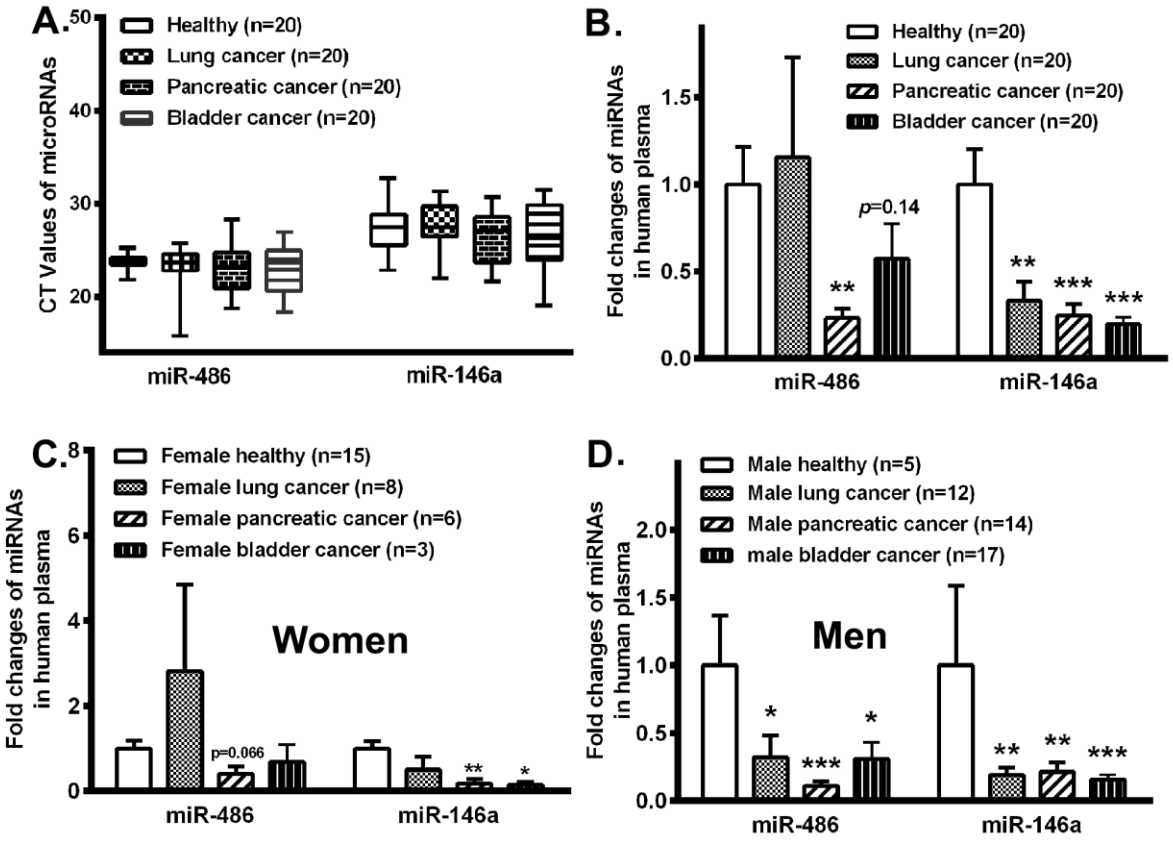

Figure 2

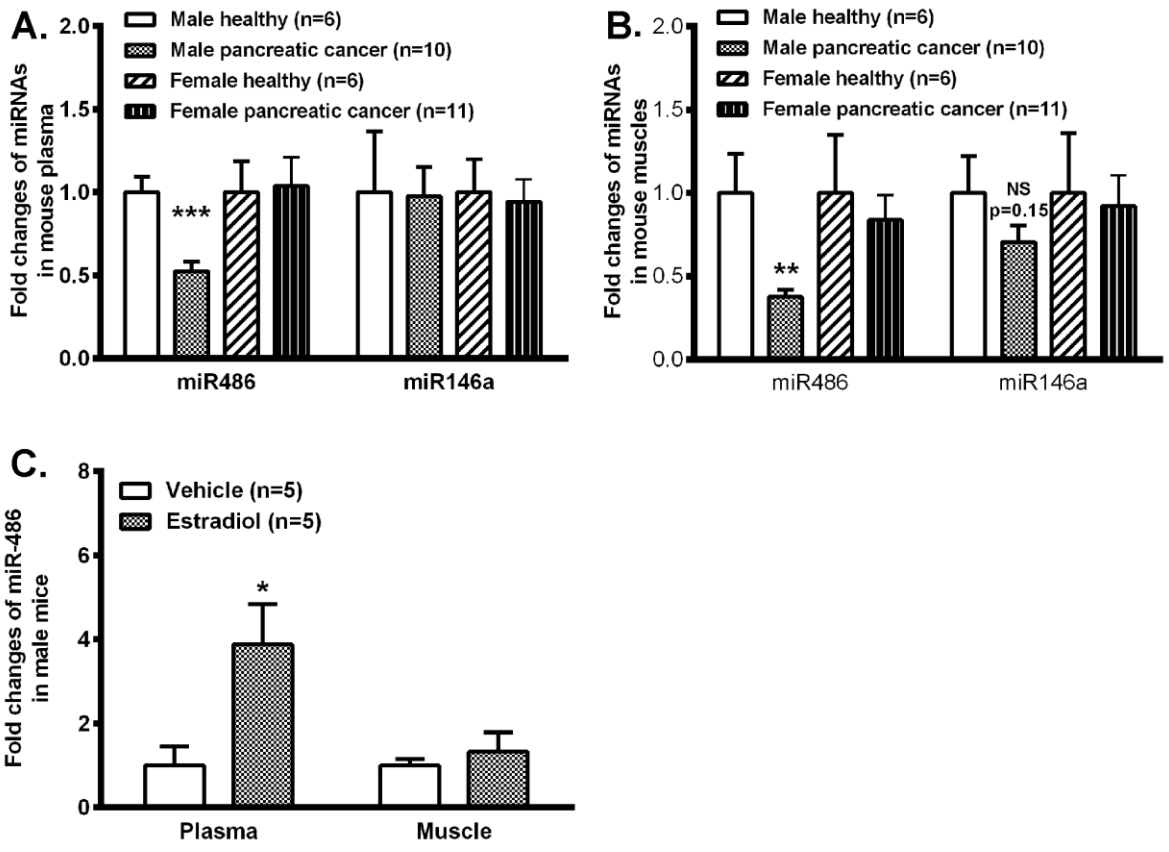

Figure 3

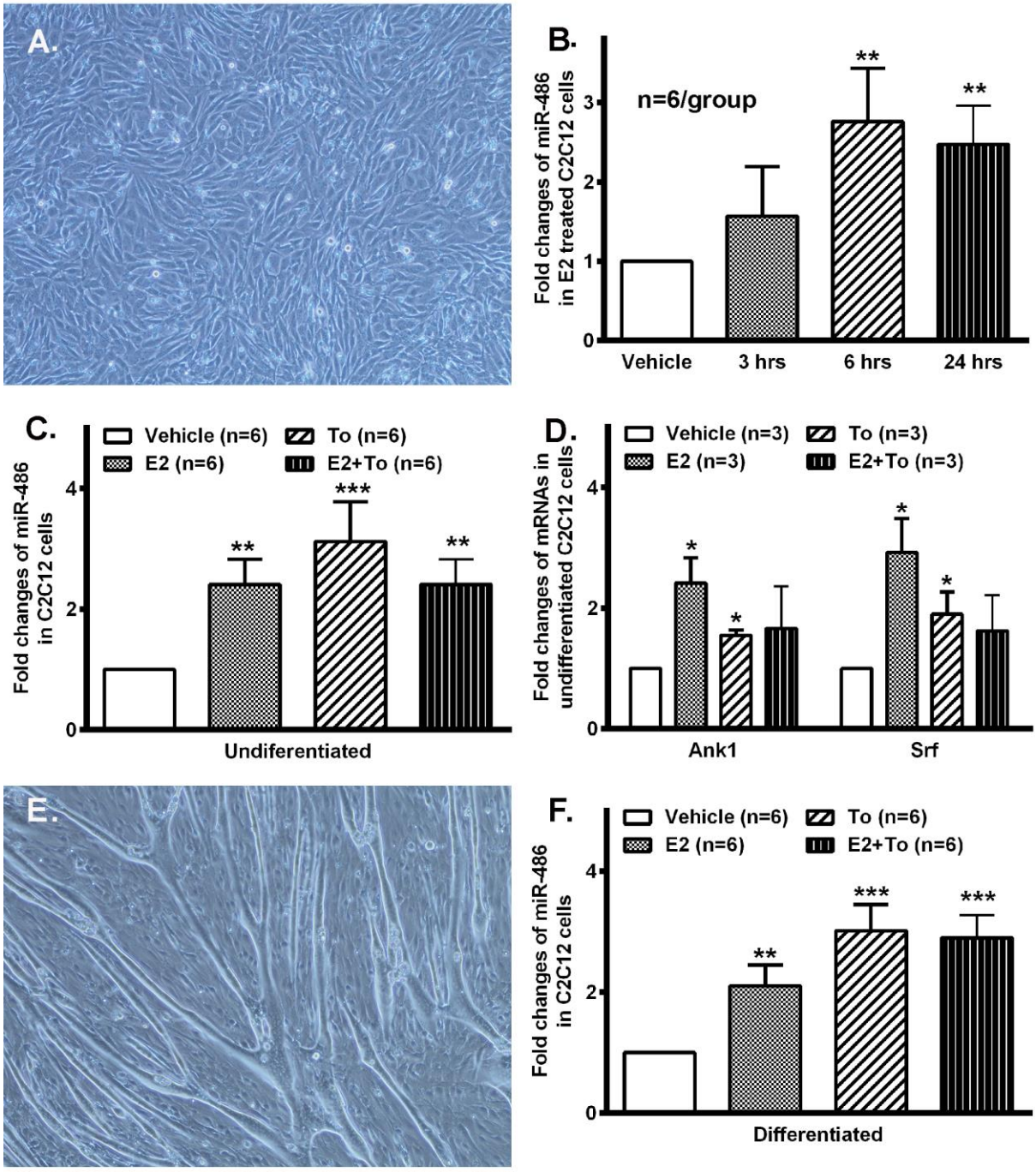

Figure 4

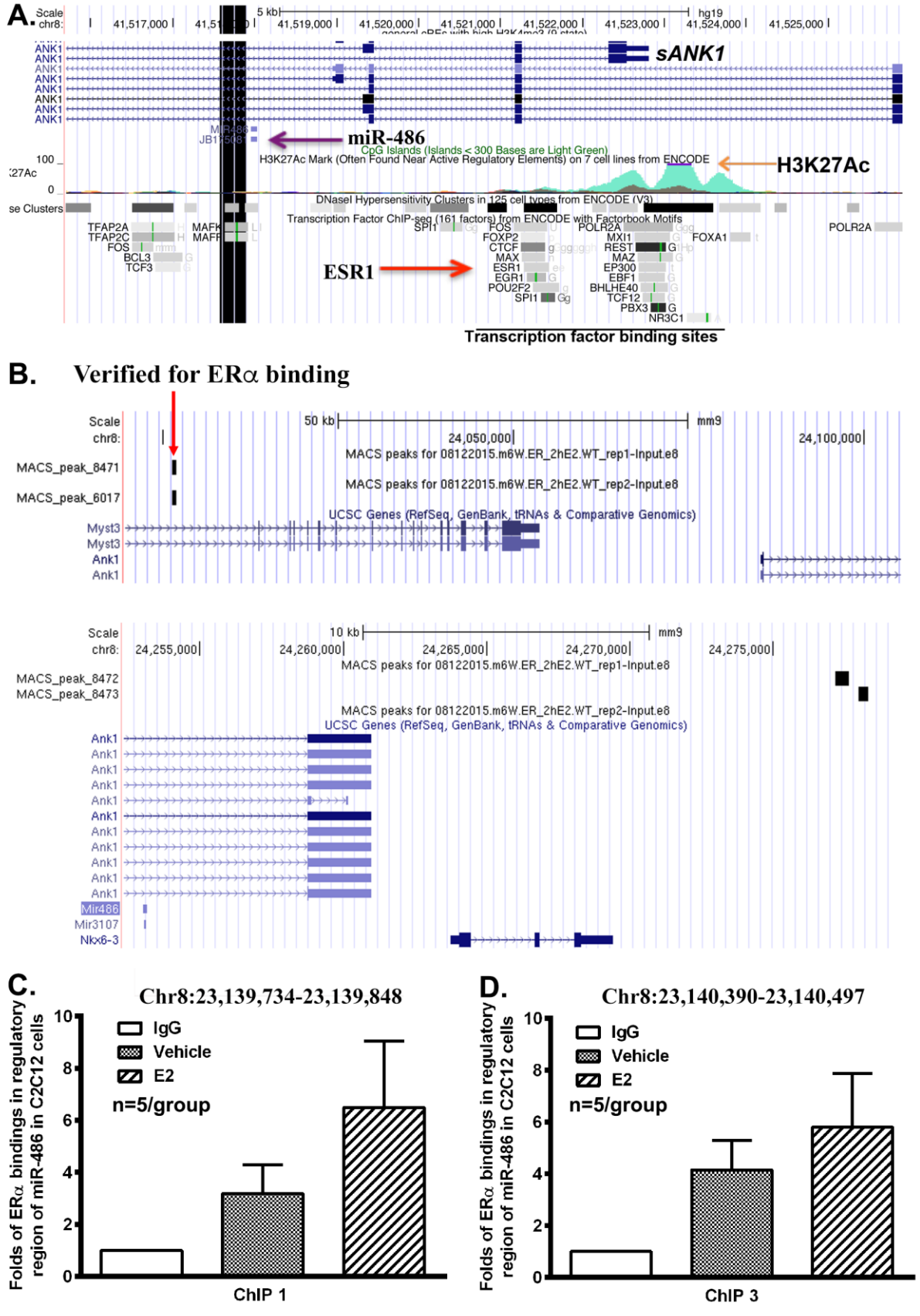

Figure 5

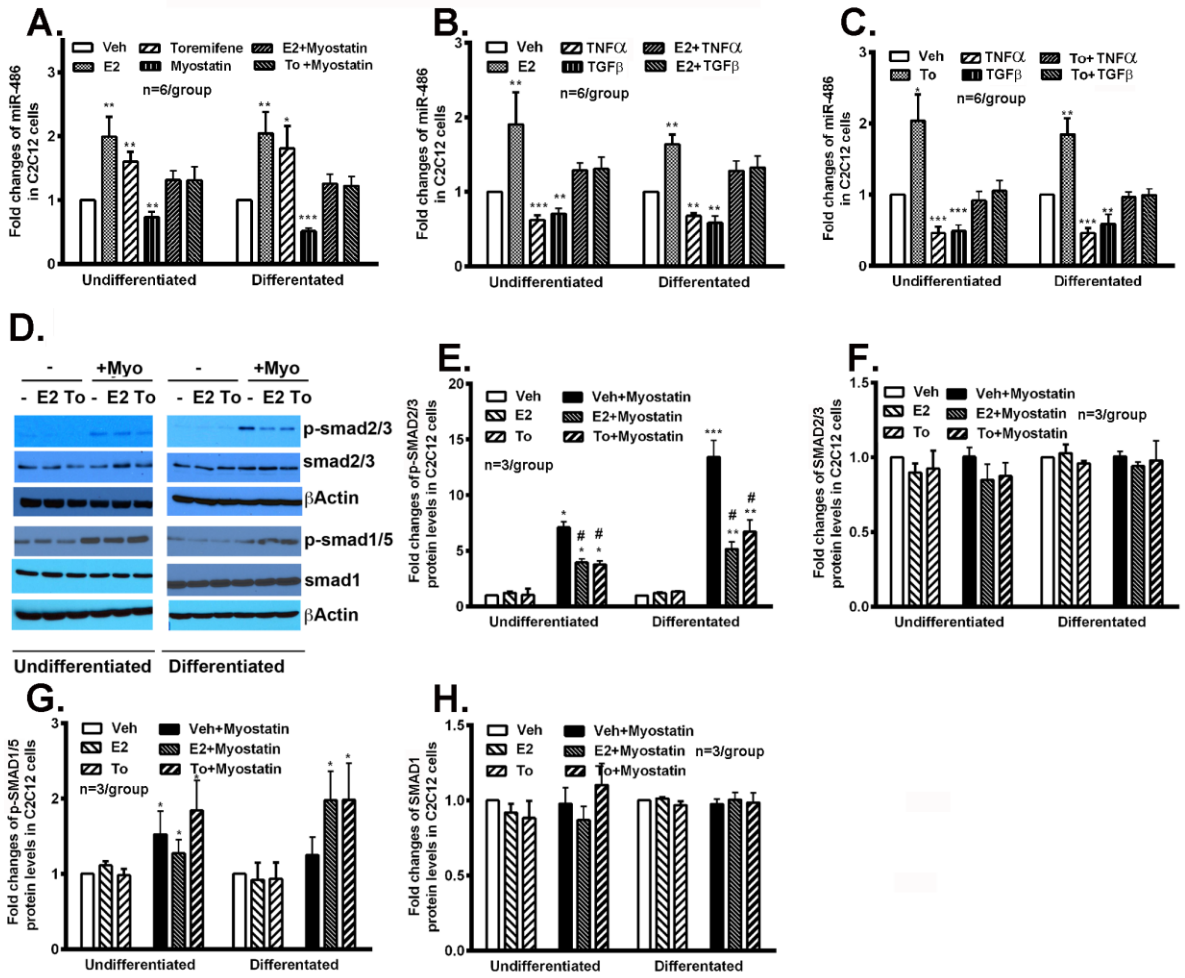

Figure 6

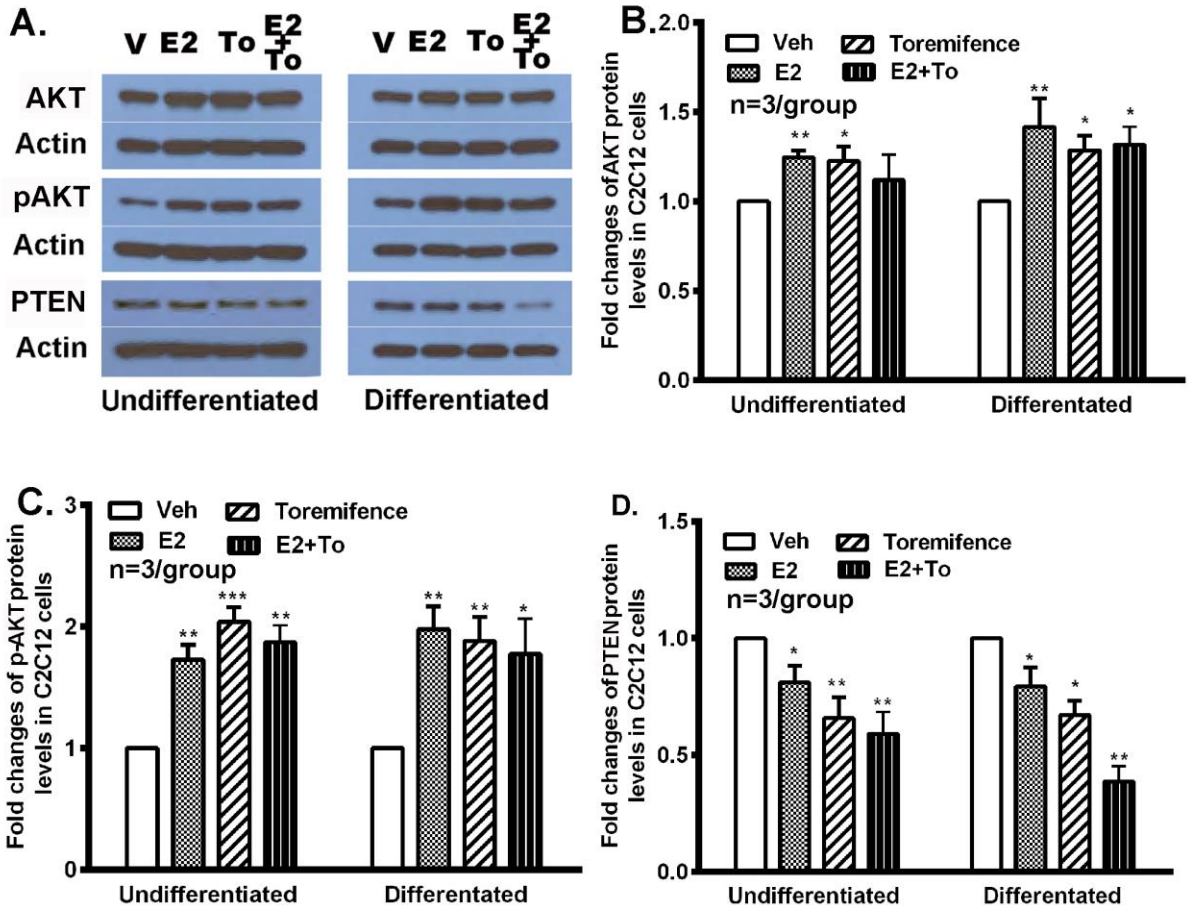

Figure 7

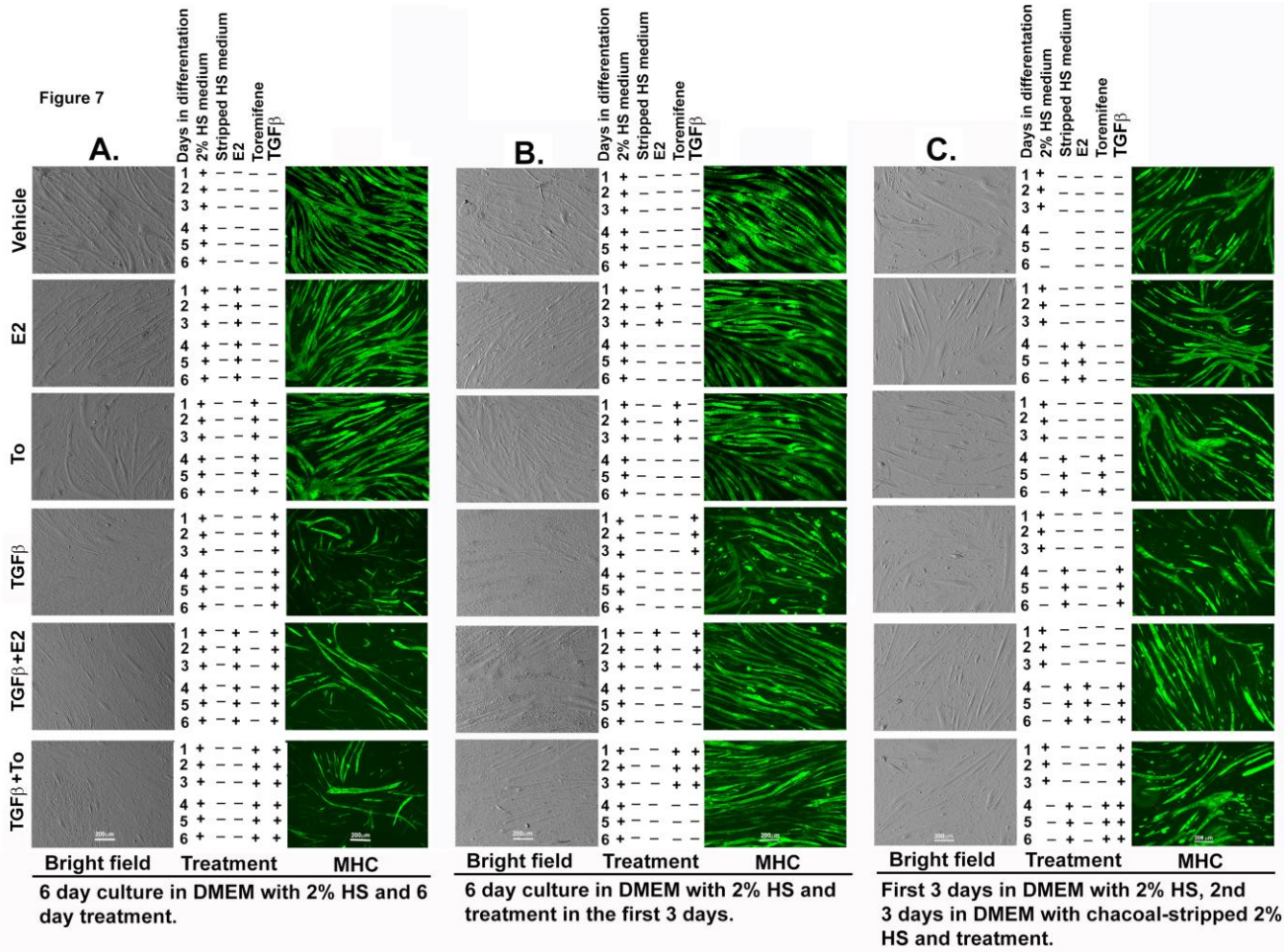

Figure 8